Journal of Biomolecular NMR, 8 (1996) 67–76
ESCOM

J-Bio NMR 351

Practical applications of time-averaged restrained molecular dynamics to ligand–receptor systems: FK506 bound to the Q50R,A95H,K98I triple mutant of FKBP-13

Christopher A. Lepre*, David A. Pearlman, Olga Futer, David J. Livingston and Jonathan M. Moore

Vertex Pharmaceuticals Inc., 130 Waverly Street, Cambridge, MA 02139-4242, U.S.A.

Received 20 December 1995
Accepted 12 March 1996

Keywords: Immunophilins; FKBP; Tacrolimus; Molecular dynamics; Structure determination

Summary

The ability of time-averaged restrained molecular dynamics (TARMD) to escape local low-energy conformations and explore conformational space is compared with conventional simulated-annealing methods. Practical suggestions are offered for performing TARMD calculations with ligand–receptor systems, and are illustrated for the complex of the immunosuppressant FK506 bound to Q50R,A95H,K98I triple mutant FKBP-13. The structure of ^{13}C-labeled FK506 bound to triple-mutant FKBP-13 was determined using a set of 87 NOE distance restraints derived from HSQC-NOESY experiments. TARMD was found to be superior to conventional simulated-annealing methods, and produced structures that were conformationally similar to FK506 bound to wild-type FKBP-12. The individual and combined effects of varying the NOE restraint force constant, using an explicit model for the protein binding pocket, and starting the calculations from different ligand conformations were explored in detail.

Introduction

Through isotope-filtered and edited methods, as well as by transferred NOE techniques, NMR spectroscopy can elucidate the conformations of bound ligands even if the structure of the protein receptor is not known. However, calculating the structure of a bound ligand is particularly challenging in the absence of information about the ligand binding pocket. In particular, care must be taken during energy-driven structure refinement to achieve adequate spatial sampling and to ensure that the resulting structures are not dominated by the force field of the ligand.

Complexes of the ^{13}C-labeled immunosuppressant FK506 (Fig. 1) with FK506-binding proteins are highly useful systems for comparing various NMR structure-refinement methods. Previous NMR studies of FK506 bound to wild-type FKBP-12 (Lepre et al., 1992) and the R42K,H87V double mutant of FKBP-12 (Lepre et al., 1994) found that the conventional restrained molecular dynamics refinement of bound FK506 structures in the absence of a model for the protein binding pocket, produced families of conformers that underrepresented the true conformational variability of the ligand and in poorly restrained regions were influenced by the force field of the free ligand. The latter studies (Lepre et al., 1994) demonstrated that time-averaged restrained molecular dynamics (TARMD) refinement of bound ligand structures increases conformational sampling and avoids problems in converting between local energy minima.

FKBP-13 belongs to the immunophilins, a family of homologous proteins that form high-affinity complexes with FK506, a potent immunosuppressant (see reviews by Schreiber et al., 1992; Sigal and Dumont, 1992; Clardy, 1994). Only one member of this family, FKBP-12 complexed with FK506, can bind and inactivate calcineurin, a Ser-Thr phosphatase that plays a key role in cytoplas-

*To whom correspondence should be addressed.

Abbreviations: DG, distance geometry; dmFKBP-12, double-mutant (R42K,H87V) FKBP-12; FKBP-12, FK506-binding protein (12 kDa); FKBP-13, FK506-binding protein (13 kDa); HSQC, heteronuclear single-quantum coherence; K_{NOE}, force constant (penalty) for NOE-derived distance restraints; MD, molecular dynamics; NOE, nuclear Overhauser effect; SA, simulated annealing; TARMD, molecular dynamics with time-averaged restraints; tmFKBP-13, triple-mutant (Q50R,A95H,K98I) FKBP-13, wtFKBP-12, wild-type FKBP-12.

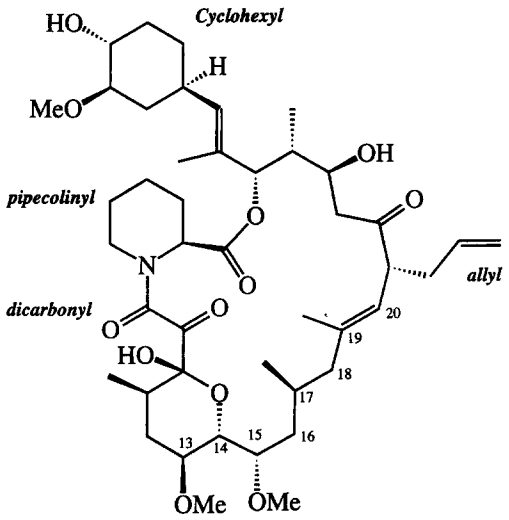

Fig. 1. Primary structure of FK506.

mic signal transduction leading to T-cell activation (Clipstone and Crabtree, 1992; O'Keefe et al., 1992). Neither FKBP-12 nor FK506 alone inhibits calcineurin (Liu et al., 1991). Extensive structural and dynamic studies have been carried out on FKBP-12 (Michnick et al., 1991; Moore et al. 1991; Cheng et al., 1993), the FK506–FKBP-12 complex (Van Duyne et al., 1991; Cheng et al., 1994), and the FK506–FKBP-12 complex bound to the A and B subunits of calcineurin (Griffith et al., 1995) with the intent of identifying unique features of the FK506 complex responsible for the inhibitory activity.

FKBP-13 is highly homologous with FKBP-12 (43% identity) and identical amino acid residues line the drug binding pocket, resulting in high FK506 binding affinity (Jin et al., 1991). In the tmFKBP-13 complex, the conformations of FK506 and the conserved binding-pocket residues are virtually identical to those observed in the wtFKBP-12 complex (Schultz et al., 1994). Despite these structural similarities, the wtFKBP-13 complex is at least a 190-fold weaker inhibitor of calcineurin (Jin et al., 1991; Futer et al., 1995), apparently due to sequence differences of several key residues in regions corresponding to the 40's and 80's loops of wtFKBP-12 (Rosen et al., 1993; Yang et al., 1993; Futer et al., 1995). When three FKBP-13 surface residues bordering the binding site are mutated (Q50R, A95H, and K98I, corresponding to R42, H87, and I90 in the FKBP-12 sequence), the FK506 complex inhibits calcineurin as well as the wtFKBP-12 complex ($K_i = 8$ nM) (Futer et al., 1995). Comparison of the X-ray structures of the FK506–FKBP-13 complexes (Schultz et al., 1994; Griffith et al., 1996) with the FK506–FKBP-12–calcineurin complex (Griffith et al., 1995) suggests that these mutations stabilize the 40's loop, remove a steric block from a groove on the surface of FKBP that contacts side chains of the B-binding helix of calcineurin A, and introduce direct electrostatic contacts required for binding (Griffith et al., 1996).

The X-ray structure of the tmFKBP-13 complex shows an interesting gap in the electron density in the C16–C18 region of the effector backbone (Griffith et al., 1996). It was proposed that this weak density arises from conformational flexibility in the effector domain that occurs in the absence of crystal contacts. At a level of 3 σ above background, either the wild-type conformation of FK506 or the distorted conformer seen in the inactive H87V,R42K FKBP-12 mutant could be contained within the density. At a level of 1 σ above background, the density more closely resembles the wild-type conformer. In the crystal, weak density may arise from either molecular mobility or static disorder. NMR studies provide a means of observing molecular mobility in solution, and in the current case show that a single conformer is preferred. The solution structure of ^{13}C-labeled FK506 bound to tmFKBP-13 is reported, and provides a well-behaved system that is used to study the abilities of various computational methods to explore conformational space using NMR-derived restraints.

Materials and Methods

Data collection and restraint generation

All data were collected at 303 K on a Bruker AMX-500 spectrometer using a sample of 2.7 mM ^{13}C-FK506–tmFKBP-13 complex in 50 mM potassium phosphate/D_2O buffer at pD 7.4. Preparation of recombinant Q50R,A95H,K98I FKBP-13 is described by Futer et al. (1995). Data were processed with Felix software (Biosym Technologies, San Diego, CA), and peak assignment and integration were carried out using the EASY program (Eccles et al., 1989). The ^{1}H and ^{13}C resonances of protein-bound ^{13}C-FK506 were assigned using ^{13}C COSY, HSQC, and HSQC-NOESY ($\tau_m = 60$ ms) spectra, as described previously (Lepre et al., 1992). The chemical shifts of the ^{1}H and ^{13}C resonances were very similar to those determined for the complex of ^{13}C-FK506 with wild-type FKBP-12 (Lepre et al., 1992).

The structure of bound FK506 was calculated using 87 NOE distance restraints derived from the 60-ms HSQC-NOESY spectrum. NOE intensities were scaled to account for the number of attached protons and the level of ^{13}C enrichment. Because ^{13}C was not incorporated biosynthetically into the pipecolinyl, there were no NOE restraints in that region. For calculations using dihedral angle restraints, six pipecolinyl-ring dihedrals were restrained to within ±60° of values consistent with the chair conformer, using a force constant of 50.0 kcal/mol rad^2. The amide linkage was not restrained in any calculation.

Structure calculations

The structure of FK506 bound to triple-mutant FKBP-13 was determined by restrained molecular dynamics, using either simulated-annealing or time-averaged

restrained MD methods. All restrained MD calculations were carried out using AMBER/SANDER 4.0 (Pearlman et al., 1995). Force-field parameters for FK506 were as previously described (Pranata and Jorgensen, 1991). All calculations were carried out in vacuo, using a distance-dependent dielectric to simulate solvent, an all-atom force field, and an 8-Å nonbonded cutoff. A time step of 2 fs was used, and the nonbonded pair list was updated every 50 steps. Bond lengths were constrained using SHAKE (Ryckaert et al., 1977). In order to prevent the ligand from drifting out of the active site during some calculations, FK506 was tethered within an explicitly modeled FKBP-13 active site by using weak (k = 1.0 kcal/mol Å^2) harmonic positional restraints applied to C8 and C9. The starting structure used was either the X-ray structure of FK506 bound to triple-mutant FKBP-13 (Griffith et al., 1996) or the NMR structure of FK506 bound to R42K,H87V FKBP-12 (Lepre et al., 1994). Two hundred independent simulated-annealing runs were carried out, starting from each ligand conformation but without using a protein model. The starting structures were energy-minimized in the presence of the NMR restraints (K_{NOE} = 20 kcal/mol Å^2), then heated linearly from 300 K to 900 K over 2 ps, while increasing the NOE force constant from 0.1 to 1.0 kcal/mol Å^2 and increasing the dihedral angle force constant from 6 to 60 kcal/mol rad^2. With the restraint force constant fixed at maximum value, the system was then allowed to equilibrate for 8 ps at 900 K, and then cooled exponentially to 300 K over 6 ps.

TARMD calculations (Torda et al., 1989,1990) were carried out using both FK506 starting structures (described above). Some runs included a protein model, and the protein was either fixed or had some residues (those contacting the ligand) that were allowed to move. The 500 ps of dynamics were carried out using $\langle r \rangle^{-1/3}$ weighting, a time step of 2 fs, and an exponential damping factor of 20 ps, as in a previous FK506 study (Pearlman, 1994). Restraint-derived forces were calculated using a pseudo-

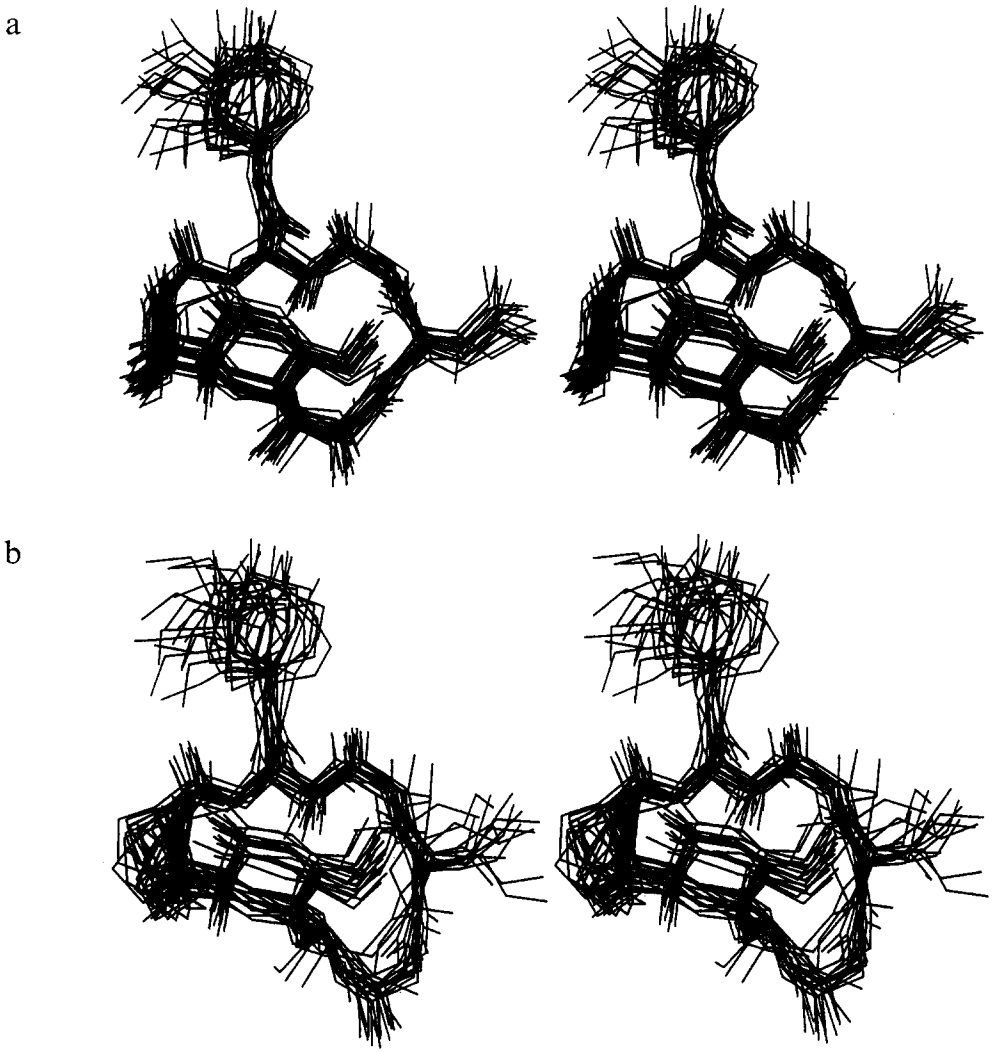

Fig. 2. Simulated-annealing structures: (a) 26 lowest-energy SA structures obtained from the tmFKBP-13 starting structure. Only heavy atoms are shown; (b) 24 lowest-energy SA structures obtained from the dmFKBP-12 starting structure. Rmsd's between starting structure and lowest-energy SA structure: tmFKBP-13 = 0.34 Å, dmFKBP-12 = 1.67 Å (based on macrocycle heavy atoms).

TABLE 1
COMPARISON OF SELECTED MACROCYCLE TORSION ANGLES IN FK506–FKBP COMPLEXES

Structure	Method	Carbons in torsion			
		C13-C14-C15-C16	C14-C15-C16-C17	C15-C16-C17-C18	C17-C18-C19-C20
wtFKBP-12	X-ray[a]	42	168	92	−100
tmFKBP-13	X-ray[b]	74	178	61	−70
	SA[c]	70	−179	57	−83
	TARMD[d]	62	176	69	−80
	TARMD[e]	67	175	68	−80
dmFKBP-12	SA[f]	−46	−87	175	−103

[a] Taken from van Duyne et al. (1991).
[b] Taken from Griffith et al. (1996).
[c] This work: lowest-energy structure obtained from simulated annealing, starting from the FK506 conformation as seen in the X-ray structure of the FKBP-13 complex.
[d] This work: average structure from a TARMD run without a protein model, starting from the FKBP-13 X-ray structure, $K_{NOE} = 1$ kcal/mol Å^2.
[e] This work: average structure from a TARMD run with the protein model, starting from the FKBP-13 X-ray structure, $K_{NOE} = 1$ kcal/mol Å^2.
[f] Taken from Lepre et al. (1994).

force formulation (Torda et al., 1990) and force constants of 0, 1.0, 4.0, 7.5, 50, or 100 kcal/mol Å^2. A temperature of about 300 K was maintained by weak coupling to an external temperature bath. The structures were saved in an archive file every 1000 steps, and the average structure was calculated by best-fitting and averaging all of the archived structures, except for those saved within the first 20 ps of the simulation (to avoid equilibration effects) (Pearlman, 1994).

Results and Discussion

Simulated-annealing structures

SA runs on FK506 alone (no bound protein) that started from the ligand conformation found in the X-ray structure of FK506 bound to tmFKBP-13 produced a well-defined family of conformers closely resembling the starting structure. Of the 200 structures calculated in this manner, the 26 having the lowest AMBER energies are shown in Fig. 2b. The lowest-energy structures have a mean pairwise rmsd of 0.77 ± 0.14 Å for all heavy atoms, and all exhibit a *trans*-amide conformation. The deviations from ideal covalent geometry are very small, as expected, since a relatively weak NOE restraint penalty (1.0 kcal/mol Å^2) was used. The rms deviation from the NOE restraints was 0.08 ± 0.03 Å.

The tmFKBP-13- and dmFKBP-12-bound conformations of FK506 differ primarily in the conformation of the C14-C20 effector region (Table 1). When the starting conformation was that of the dmFKBP-12-bound ligand, simulated annealing was unable to access the tmFKBP-13 final NMR conformation. These SA runs formed a less well ordered family of structures (average pairwise rmsd = 1.20 ± 0.45 Å) that differed in the conformation of the effector region (Fig. 2a) and had higher restraint violations (rms violation of 0.34 Å). Higher NOE force constants (4 and 10 kcal/mol Å^2) produced the same result, but with higher violation energies. At 60 kcal/mol Å^2, the system became unstable, as reflected by the high temperature and kinetic energy, and distortions of the covalent geometry. In an effort to achieve better conformational sampling, the maximum temperature of the simulated-annealing protocol was changed from 900 K to 1500 K and the force constant was kept low ($K_{NOE} = 1$ kcal/mol Å^2). The structures produced by this high-temperature protocol, however, still did not converge to a well-defined family (the 23 lowest-energy structures had a mean pairwise rmsd of 1.97 ± 0.47 Å), exhibited higher restraint violation energies, and did not adopt the tmFKBP-13-like conformation.

The failure of simulated annealing to sample effector region conformations that are significantly different from the dmFKBP-12 starting conformer appears to be due to the presence of a local energy minimum, which arises because the transient violations of the NOE distance restraints necessary for the macrocycle to reorient itself give rise to an energy barrier that cannot be overcome by the kinetic energy. In order to test this premise, unrestrained MD runs were carried out for 500 ps at 300, 400, 500, 1000, and 1500 K, respectively, starting from the double-mutant-bound conformation of FK506 with no protein model. At 300 K, the ligand remained in the starting conformation for the entire run. At 400 K, the ligand switched over to the tmFKBP-13-bound conformation after 360 ps. At 500 K, the ligand exchanged freely between the two conformations, and at 1000 K and above it was highly disordered. These simulations, combined with an analysis of the potential energy as a function of the effector torsion O4-C12-C13-C14 (Itoh et al., 1995), indicate that the major experimentally observed conformers represent two energy minima that are separated by an estimated barrier of 6–11 kcal/mole, with the tmFKBP-13-bound conformer slightly lower in energy.

In this case, the transition state between the low-energy conformers results in large restraint violations, so that rather than induce the structure to move from one energy

well to another, higher NOE force constants effectively raise the energy barrier between the conformers. Conventional distance-geometry/MD refinement methods, which are not dependent upon a starting structure and generate conformers on both sides of the barrier, could be used to circumvent this problem, and in fact produce a family of structures that resemble the SA structures of Fig. 2b (data not shown). Another method that avoids problems with large restraint-induced barriers between local minima is MD with time-averaged distance restraints (TARMD). TARMD has an added advantage over DG of reflecting the intrinsically time-averaged nature of the experimentally derived distance restraints. The results of the TARMD approach are described in detail later in this paper.

Overall, the SA structure of FK506 bound to tmFKBP-13 resembles the conformation seen in the X-ray structure (Griffith et al., 1996) (Fig. 3) with an rmsd between the X-ray and NMR structures of 0.34 Å for macrocycle heavy atoms (determined using the lowest-energy structure). Macrocycle torsion angles in the effector region (Table 1) are within 13° of one another. The conformation also resembles that of FK506 bound to wild-type FKBP-12 (rmsd = 0.37 Å) (Van Duyne et al., 1991), though some torsions differ by up to 30°. Reflecting this similarity, the proton chemical shifts of the ligand in the tmFKBP-13 complex are all within ±0.03 ppm of those observed for FK506 bound to wtFKBP-12 (Lepre et al., 1992).

On the basis of previous NMR studies, the allyl group is expected to be exposed to the solvent on the surface of the complex (Lepre et al., 1992,1993). As observed previously, the NOE intensities for this region are weak and the resonance line widths are narrow, indicating that it is highly mobile. As a result, the allyl group is the most highly disordered region of the bound ligand in all of the calculated structures.

Time-averaged restrained MD calculations

In a previous study of FK506 bound to dmFKBP-12, simulated-annealing runs that started from the wild-type conformation of FK506 docked onto the double-mutant protein pocket became trapped in a higher-energy minimum (Lepre et al., 1994). TARMD calculations succeeded in overcoming the local energy barrier, and the ligand converted to a final low-energy conformation that differed significantly from the starting structure, particularly in the effector region.

In the present work, the use of TARMD to force the conversion between various FK506 conformers has been studied by systematically changing the NOE restraint penalty, the starting conformation, and the model for the protein binding pocket. The exponential damping factor was not varied, since a suitable value of this parameter was previously determined in an independent set of FK506 simulations (Pearlman, 1994). The results of 25 independent TARMD runs are presented in Fig. 4 as a matrix of structure ensembles.

Effect of varying the restraint penalty

In simulated-annealing calculations, increasing the NOE restraint penalty typically results in a family of structures with lower rmsd's. In TARMD calculations, the opposite is generally true: a higher NOE penalty causes restraint violations to be corrected by a correspondingly higher force, leading to higher velocities and thus higher rmsd's in the family of snapshots assembled over the course of the run (Pearlman, 1994). In the first column of the TARMD results matrix (Fig. 4) it can be seen that in this case increasing K_{NOE} from 1 to 7.5 kcal/mol Å^2 does not, however, significantly increase the rmsd's. This unresponsiveness of rmsd to the value of K_{NOE} appears to be due to the relatively small number of restraint violations in the tmFKBP-13 starting structure. In support of this notion, increasing the NOE restraint penalty from 1 to 4 kcal/mol Å^2 raises the total energy by only 14 kcal/mol when using the tmFKBP-13 starting structure, but the energy increases by 95 kcal/mol when using the dmFKBP-12 conformer (which has larger average violations). Because time-averaged restraints are not conservative, they can cause heating of the system (Torda et al., 1990). As a result, at a restraint penalty of 50 kcal/mol Å^2, the temperature of the system becomes unstable (i.e., it increases and fluctuates), and the family of structures is disordered.

Effect of the protein model

The effects of including a crystallographic model for the protein pocket (Griffith et al., 1996) in the TARMD calculations may be examined by comparing the first and second columns of the TARMD results matrix (Fig. 4). The average structures obtained if the protein was included were similar to those obtained without the protein (heavy atom rmsd = 0.54 Å at K_{NOE} = 7.5 kcal/mol Å^2). The most pronounced effect of the protein binding pocket is to limit the amplitude of ligand motions. When the protein model is used, the rmsd's are uniformly low for all parts of the ligand, except for those that are not in contact with the protein, such as the allyl and the solvent-exposed edge of the cyclohexyl moiety. For example, the pipecolinyl ring has no NOE restraints, and hence is poorly defined in structures determined without the protein model (first column in Fig. 4). When the model is used, this ring is the most deeply buried part of the ligand and it becomes well-ordered (second column). Interestingly, the motional limiting effect also prevents the system from becoming unstable at K_{NOE} = 50 kcal/mol Å^2.

In theory, limiting the motions of the previously unrestrained pipecolinyl group by using the protein model could cause higher temperatures elsewhere in the molecule. Because the scaling factor for coupling to the external

temperature bath is based upon the average temperature, cooling of some regions by restricting motions allows higher temperatures elsewhere while maintaining the same average, possibly resulting in higher restraint violations. This effect was not observed in the current study. On the other hand, if the force field associated with the unbound ligand is a poor model for the protein–ligand complex, then inclusion of a protein in the model may stabilize conformers which satisfy the restraints, but yet are high in energy in the model lacking a protein. As a result, we observe that the ligand has both better nonbonded energies and lower restraint violations when bound to the protein model.

Use of the protein model lowered the average energy of the structures during the TARMD trajectory by approximately 17 kcal/mol (Table 2). The FK506 geometry was more strained if the protein was present, but favorable nonbonded contacts more than compensated for the added covalent strain. The violation energy was also lower, hence the protein-bound conformers were not only stabilized by the protein, and they better satisfied the NOE restraints. The average structures obtained with and without the protein model were most similar in the effector region (dihedrals within 5°, Table 1), and most different in the cyclohexyl and pipecolinyl regions (both of which are poorly restrained and contact the protein).

In addition, a parallel series of TARMD calculations was carried out in which the residues contacting the ligand in the binding pocket of tmFKBP-13 (Y16, F26, D27, F36, V45, I46, W49, I66, Y72, H77, F89, I99) (Griffith et al., 1996) were allowed to move during the run. As shown in Fig. 4, the results were identical to those obtained when the ligand binding residues were fixed.

Effect of starting conformation

When the starting and final conformations are relatively similar, TARMD readily produces a family of conformers centered about the 'correct' final structure. For example, TARMD runs starting from the closely related wtFKBP-12- and tmFKBP-13-bound conformations yielded identical average structures, (effector region rmsd's = 0.14 Å, effector dihedrals within 10° (data not shown)). When the starting and final structures are significantly different, however, the ability of TARMD to convert the starting conformer to other geometry depends partly upon the value of the restraint penalty, with larger values producing better conformational sampling.

This phenomenon is illustrated in Fig. 4. When the starting structure (no protein model) was the tmFKBP-13 conformer (column 1), essentially the same family of structures resulted for any value of K_{NOE} from 1 to 7.5 kcal/mol Å^2. In contrast, when the starting structure was the dmFKBP-12 conformer (column 4), the resulting family of TARMD structures was intermediate between the dmFKBP-12 and tmFKBP-13 conformers at low K_{NOE} (1 and 4 kcal/mol Å^2), but resembled the tmFKBP-13 conformer at higher K_{NOE} (7.5 kcal/mol Å^2). The energy increases by 85 kcal/mol if the K_{NOE} value is increased from 1 to 4 kcal/mol Å^2, due to increasing the restraint-violation and covalent-strain energies, and this increase is reflected by larger rmsd's in the family of structures. The families obtained with a K_{NOE} value of 1 and 4 kcal/mol Å^2 exhibit intermediate values for the dihedral angles in the

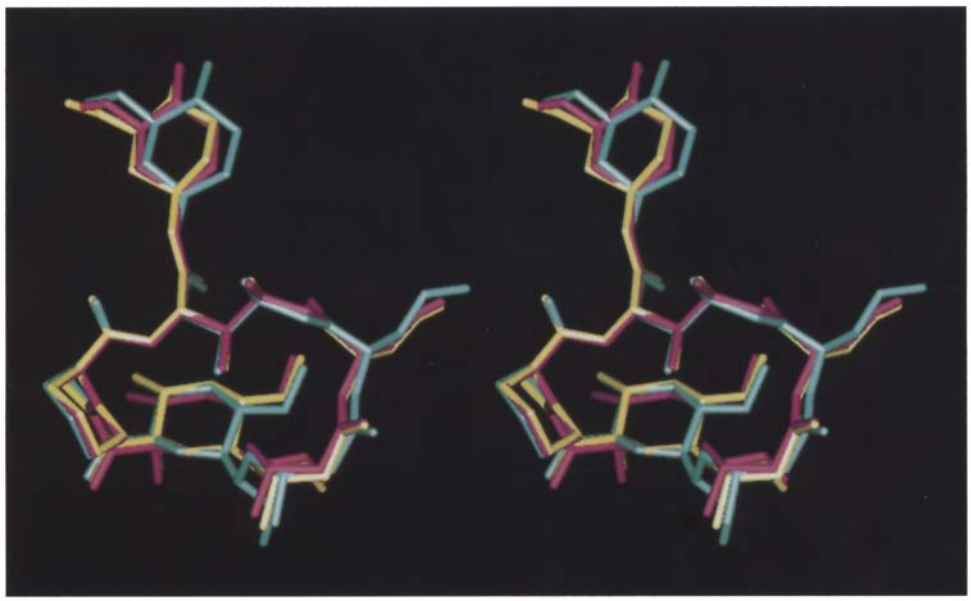

Fig. 3. Comparison of tmFKBP-13-bound structures: (cyan) structure of FK506 found in the X-ray structure of the tmFKBP-13 complex (Griffith et al., 1996); (yellow) average structure from TARMD, starting from the tmFKBP-13 conformer and using the tmFKBP-13 protein model with K_{NOE} = 7.5 kcal/mol Å^2; (magenta) average structure from TARMD, starting from the dmFKBP-12 conformer and using the dmFKBP-12 protein model with K_{NOE} = 7.5 kcal/mol Å^2. Superposition is based on all heavy atoms.

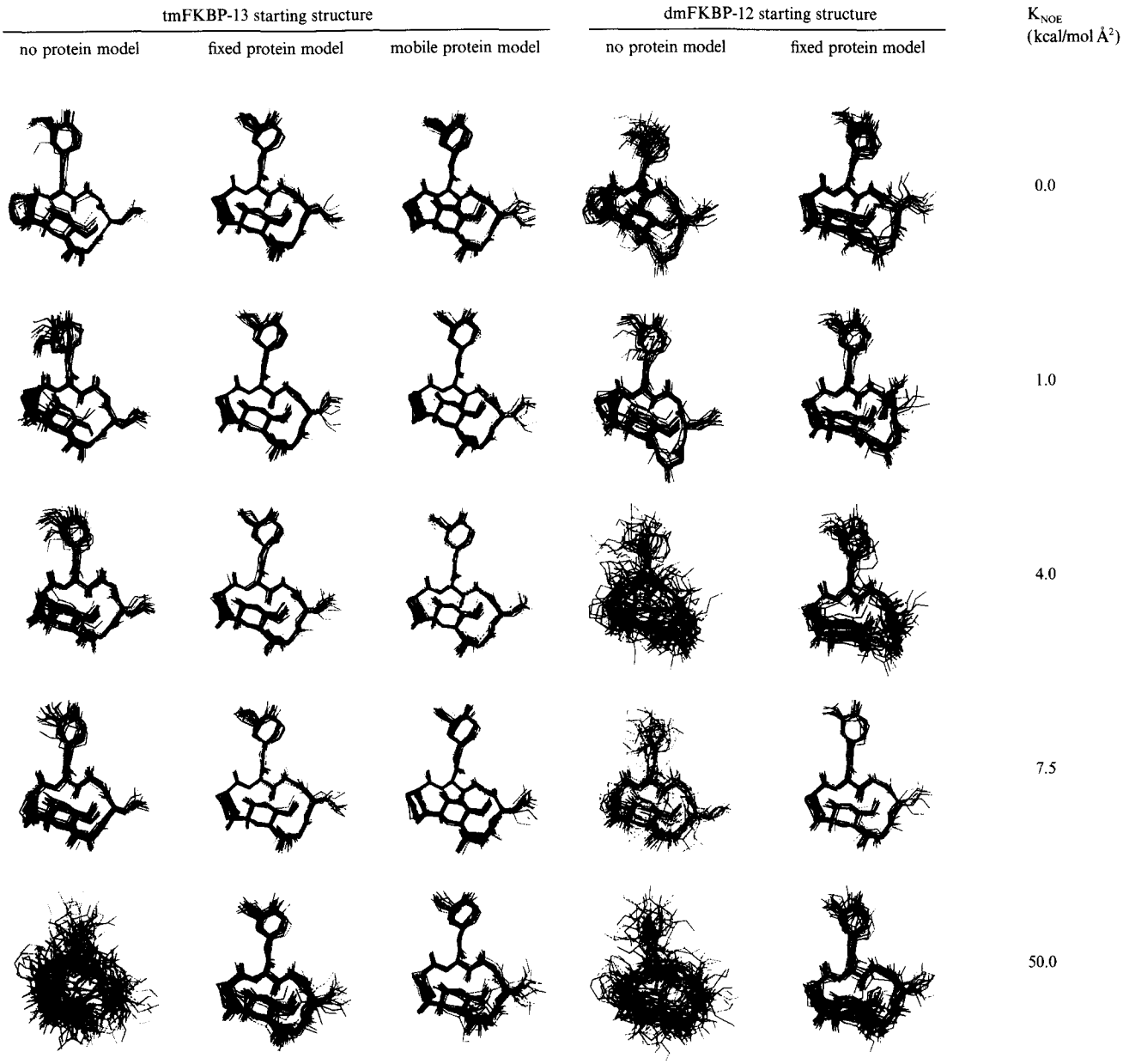

Fig. 4. Matrix representation of TARMD results. Families of 25 structures sampled during the course of 500-ps runs at 300 K, heavy-atom superposition. Horizontal axis: the starting structure for the TARMD runs was varied, starting from either the tmFKBP-13 or dmFKBP-12 conformer and employing the no-protein model, a model in which all protein atoms were fixed, or a model in which residues contacting the ligand were mobile. Vertical axis: NOE-derived restraint penalty (K_{NOE}) varied from 0 to 50 kcal/mol Å^2.

effector region of the macrocycle, and the 15-MeO group is on the same side of the plane defined by the macrocycle ring as in the dmFKBP-12 conformer. These intermediate structures resemble the family of 'trapped' SA structures shown in Fig. 2b. At $K_{NOE} = 7.5$ kcal/mol Å^2, the potential energy and the rmsd's of the family are lower, the 15-MeO group has switched over to the opposite side of macrocycle, and the effector dihedrals are close to the tmFKBP-13 conformer values (although high rmsd's preclude precise quantification).

Although the dmFKBP-12 starting structure converts spontaneously to the tmFKBP-13 conformer during unrestrained MD runs at higher temperatures, the conversion observed in the restrained runs is not a consequence of a low density of restraints in the effector region. The effector is in fact the most heavily restrained portion of the molecule. The dependence of the conversion upon K_{NOE} demonstrates that it is actually driven by the experimental restraints.

Unrestrained MD runs reveal that if the protein is not included in the calculations, the dmFKBP-12 conformer is ca. 60 kcal/mol more strained than the tmFKBP-13 conformer (Table 2). This covalent strain may be responsible for the larger rmsd's observed for the unrestrained dmFKBP-12 family of MD structures (row 1, column 4 in Fig. 4). When the protein is included (row 1, column 5),

TABLE 2
AVERAGE LIGAND ENERGIES FROM TARMD RUNS

Protein	K_{NOE} (kcal/mol Å^2)	Ligand energy (kcal/mol)				
		E_{AMBER} [a]	$E_{restraint}$	E_{angle}	$E_{dihedral}$	$E_{nonbond}$
tmFKBP-13						
no model	0	-31.3	-[b]	13.7	21.4	-34.0
	1.0	-28.1	5.6	16.8	24.7	-38.4
with model	0	-45.8	-	64.2	23.9	-97.6
	1.0	-44.8	1.2	65.0	23.2	-97.3
dmFKBP-12						
no model	0	56.6	-	60.1	35.2	-33.3
	1.0	-23.5	10.3	14.4	25.7	-36.8
with model	0	-28.3	-	62.4	26.9	-88.7
	1.0	-16.8	8.3	67.3	29.3	-88.9
	7.5	-28.7	1.4	65.0	25.6	-91.7

Averages were calculated from results of the final 100 ps of the runs.
[a] E_{AMBER} is the potential energy, exclusive of the restraint energy.
[b] Not applicable for unrestrained runs.

the strain energy of the unrestrained tmFKBP-13 conformer is as high as for the dmFKBP-12 conformer, but because it is better stabilized by nonbonded interactions, its overall energy is lower by approximately 17 kcal/mol.

Use of the protein model in restrained TARMD calculations allows the two conformers to be better distinguished energetically than is possible in calculations carried out with the ligand alone. When no protein is present and $K_{NOE} = 1$ kcal/mol Å^2, the average energies measured during TARMD are essentially the same regardless of the starting conformer, except for the restraint violation energy, which is 5 kcal/mol higher for the dmFKBP-12 case (Table 2). When the protein is present, the restraint violation energies are lower for both conformers. The intermediate structures produced by the dmFKBP-12 starting conformer at $K_{NOE} = 1$ kcal/mol Å^2 are covalently strained and have 6 kcal/mol higher average violation energies than the tmFKBP-13 conformer, making their average AMBER energy higher by 26 kcal/mol. Thus, when the tmFKBP-13 starting structure is refined with the protein model, the resulting structures are not only lower in energy than those obtained starting from the dmFKBP-12 conformer, but they also satisfy the restraints better than calculations using the tmFKBP-13 starting structure and no protein model.

When the dmFKBP-12 starting structure is refined using the protein model, increasing the K_{NOE} value increases the AMBER energy up to 4 kcal/mol, but for higher K_{NOE} values the AMBER energy abruptly drops by 12 kcal/mol and the structures adopt the tmFKBP-13 conformation (row 4, column 5 in Fig. 4). This decrease is due to a lower restraint energy, reduced covalent strain, and better nonbonded interactions. The presence of a protein doesn't appear to change the value of K_{NOE} at which the tmFKBP-13 conformer is accessed (i.e., the barrier to conversion between the two conformers is unchanged).

Conclusions

The NMR structure of FK506 bound to tmFKBP-13 is very similar to that found for FK506 bound to wtFKBP-12. Since the conformation of FK506 bound in the inactive wild-type FKBP-13 complex also resembles the highly active wtFKBP-12 conformer (Schultz et al., 1994), it is clear that the FKBP-13 loop mutations confer their activity by restoring direct interactions with calcineurin rather than by altering the ligand conformation.

Previous comparisons of NMR and X-ray structures of FK506–FKBP complexes identified differences attributed to crystal-packing interactions by the surface-exposed FK506 effector region (Lepre et al., 1992,1994). In contrast, the X-ray structure of the tmFKBP-13 complex (Griffith et al., 1996) exhibits only one intermolecular contact in the effector region (at the tip of the allyl group), and agrees well with the NMR structure. This result supports the previous conclusion that X-ray structures of FK506–FKBP complexes which exhibit crystal contacts in the effector region should be interpreted cautiously, unless other confirmatory data are available (Lepre et al., 1992).

Crystallographic and NMR studies of FK506–FKBP-12 complexes have identified two ligand conformers: a wild-type-like conformer that inhibits calcineurin, and an energetically similar but inactive 'alternate' conformation, adopted when bound to dmFKBP-12. TARMD analysis of our NMR data shows that both conformers are of reasonable energy and the barrier between them is traversable by TARMD, with the wild-type-like conformer preferred in the tmFKBP-13 complex. Since only a single set of resonances is observed in the NOE spectra, either one conformer predominates, or the effector region of the bound ligand undergoes fast exchange between the two predominant conformers at room temperature, giving

averaged chemical shifts. Although the latter conclusion is suggested by the observation of weak electron density in the effector region of the tmFKBP-13 complex (Griffith et al., 1996), the similarity between the chemical shifts and line widths of the wtFKBP-12 and tmFKBP-13 complexes supports the idea that a single, wild-type-like conformer predominates.

In this application, TARMD methods have proved to be superior to conventional simulated-annealing protocols for exploring conformational space and avoiding local minima. Based upon our experience, the following practical suggestions are offered for optimizing the results of TARMD calculations:

(i) a series of TARMD calculations should be run with varying restraint force constants. In practice, the K_{NOE} value can be adjusted in order to achieve the desired level of conformational sampling, up to the limit at which the system becomes unstable. Our preference is to use the minimum force constant that gives satisfactory conformational sampling and introduces no covalent violations. For example, a value of $K_{NOE} = 1$ kcal/mol Å^2 produced an ensemble with an rmsd most similar to the unrestrained MD runs and is therefore probably the best representation of the data;

(ii) if available, an explicit model should be employed for the protein binding site. If the protein model is appropriate, then the restraints will generally be better satisfied when the model is used. The violations of average structures are not valid for comparison, since the average structures may contain larger restraint violations than the individual members of the ensemble;

(iii) conformational space can best be explored by starting the TARMD from different conformers. These starting conformers can be generated by conventional methods (such as DG) that are highly efficient in generating structures. Ideally, subsequent TARMD refinement should produce a common family, with a concomitant decrease in violation and covalent strain energies, provided that the energy of the system is sufficient to cross over the barriers between conformers;

(iv) in this application, TARMD is used as a tool for sampling conformational space in structure calculations, and isn't intended to accurately represent the amplitudes or time scales of molecular motions. Motional amplitudes will be enhanced and conformational interconversion times reduced, because the simulations are run in vacuo (Torda et al., 1990). Attention to the exponential damping factor is essential, since large domain motions that equilibrate on time scales longer than the averaging period (20 ps in this work) may be frozen out (Scheek et al., 1995). If information about molecular motions is sought, then we suggest that TARMD be initially performed with higher restraint weights in order to ensure that conformational space is adequately sampled and a 'converged' structure is found. A subsequent TARMD run may then be carried out starting from the converged structure, with lower restraint weights and a longer averaging period, in order to probe the motional properties of the molecule.

In this instance, conventional distance-geometry/MD methods were successful in producing essentially the same solution structure as TARMD methods, as do other methods employing random starting coordinates. The TARMD approach, however, accounts for motional averaging of the NOEs and allows identification of multiple, interconvertible species that may contribute to the conformational disorder observed crystallographically. Thus, although other conventional methods are certainly adequate for determining the 'correct' structure, TARMD analysis offers additional insight into the possible dynamic processes of the bound ligand.

Acknowledgements

^{13}C-labeled FK506 was produced by H. Kuboniwa and K. Munemura of Chugai Pharmaceutical Co., Ltd.. We wish to thank J. Griffith and M. Navia for providing crystallographic data prior to publication and for useful discussions.

References

Cheng, J.-W., Lepre, C.A., Chambers, S., Fulghum, J.R., Thomson, J.A. and Moore, J.M. (1993) *Biochemistry*, **32**, 9000–9010.

Cheng, J.-W., Lepre, C.A. and Moore, J.M. (1994) *Biochemistry*, **33**, 4093–4100.

Clardy, J. (1994) *Perspect. Drug Discov. Design*, **2**, 124–144.

Clipstone, N.A. and Crabtree, G.R. (1992) *Nature*, **357**, 695–697.

Eccles, C., Billeter, M., Güntert, P. and Wüthrich, K. (1989) *Abstracts for the Xth Meeting of the International Society for Magnetic Resonance*, Morzine, France, July 16–21, p. S50.

Futer, O., DeCenzo, M.T., Park, S., Jarrett, B., Aldape, R. and Livingston, D.J. (1995) *J. Biol. Chem.*, **270**, 18935–18940.

Griffith, J.P., Kim, J.L., Kim, E.E., Sintchak, M.D., Thomson, J.A., Fitzgibbon, M.J., Fleming, M.A., Caron, P.A., Hsiao, K. and Navia, M.A. (1995) *Cell*, **82**, 507–522.

Griffith, J.P. (1996) personal communication.

Itoh, S., DeCenzo, M.T., Livingston, D.J., Pearlman, D.A. and Navia, M. (1995) *Bioorg. Med. Chem. Lett.*, **5**, 1983–1988.

Jin, Y.-J., Albers, M.W., Lane, W.S., Bierer, B.E., Schreiber, S.L. and Burakoff, S.J. (1991) *Proc. Natl. Acad. Sci. USA*, **88**, 6677–6681.

Liu, J., Albers, M.W., Wandless, T.J., Luan, S., Alberg, D.G., Belshaw, P.J., Cohen, P., Meadows, R.P., Nettesheim, D.G., Xu, R.X., Olejniczak, E.T., Petros, A.M., Holzman, T.F., Michnick, S.W., Rosen, M.K., Wandless, T.J., Karplus, M. and Schreiber, S.L. (1991) *Science*, **252**, 836.

Lepre, C.A., Thomson, J.A. and Moore, J.M. (1992) *Febs Lett.*, **1**, 89–96.

Lepre, C.A., Cheng, J-W and Moore, J.M. (1993) *J. Am. Chem. Soc.*, **115**, 4929–4930.

Lepre, C.A., Pearlman, D.A., Cheng, J.-W., DeCenzo, M.T., Livingston, D.J. and Moore, J.M. (1994) *Biochemistry*, **33**, 13571–13580.

Liu, J., Farmer, J.D.J., Lane, W.S., Friedman, J., Weissman, I. and Schreiber, S.L. (1991) *Cell*, **66**, 807–815.

Michnick, S.W., Rosen, M.K., Wandless, T.J., Karplus, P.A. and Schreiber, S.L. (1991) *Science*, **251**, 836–839.

Moore, J.M., Peattie, D.A., Fitzgibbon, M.J. and Thomson, J.A. (1991) *Nature*, **351**, 248–250.

Pearlman, D.A., Case, D.A., Caldwell, J.C., Ross, W.S., Cheatham, T.C., De Bolt, S.E., Ferguson, D.M., Seibel, G.L. and Kollman, P.A. (1995) *Comput. Phys. Commun.*, **91**, 1–41.

Pearlman, D.A. (1994) *J. Biomol. NMR*, **4**, 1–16.

O'Keefe, S.J., Tamura, J., Kincaid, R.L., Tocci, M.J., O'Neill, E.A. (1992) *Nature*, **357**, 692–694.

Pranata, J. and Jorgensen, W.L. (1991) *J. Am. Chem. Soc.*, **113**, 9483–9493.

Rosen, M.K., Yang, D., Martin, P.K. and Schreiber, S.L. (1993) *J. Am. Chem. Soc.*, **115**, 821–822.

Ryckaert, J.P., Ciccotti, G. and Berendsen, H.J.C. (1997) *J. Comput. Phys.*, **23**, 327–341.

Scheek, R.M., Van Nuland, V.A.J., De Groot, B.L. and Amadei, A. (1995) *J. Biomol. NMR*, **5**, 106–111.

Schreiber, S.L., Liu, J., Albers, M.W., Rosen, M.K., Standaert, R.F., Wandless, T.J., Somers, P.K. (1992) *Tetrahedron*, **48**, 2545–2558.

Schultz, L.W., Martin, P.K., Liang, J., Schrieber, S.L. and Clardy, J. (1994) *J. Am. Chem. Soc.*, **116**, 3129–3130.

Sigal, N.H. and Dumont, F.J. (1992) *Annu. Rev. Immunol.*, **10**, 519–560.

Torda, A.E., Scheek, R.M. and Van Gunsteren, W.F. (1989) *Chem. Phys. Lett.*, **157**, 289–294.

Torda, A.E., Scheek, R.M. and Van Gunsteren, W.F. (1990) *J. Mol. Biol.*, **214**, 223–235.

Van Duyne, G.D., Standaert, R.F., Karplus, P.A., Schreiber, S.L. and Clardy, J. (1991) *Science*, **252**, 839.

Yang, D., Rosen, M.K. and Schreiber, S.L. (1993) *J. Am. Chem. Soc.*, **115**, 819–820.